# Accuracy of Directional Spectrum Estimation in 2nd Order Multidirectional Waves

Iversen, Sarah Krogh; Andersen, Thomas Lykke; Frigaard, Peter

*Published in:*
Proceedings of the Thirty-third (2023) International Ocean and Polar Engineering Conference

*Publication date:*
2023

*Document Version*
Accepted author manuscript, peer reviewed version

# Accuracy of Directional Spectrum Estimation in 2nd Order Multidirectional Waves

*Sarah Krogh Iversen, Thomas Lykke Andersen & Peter Frigaard*
Department of the Built Environment, Aalborg University
Aalborg, Denmark

## ABSTRACT

For design validation of offshore structures and conceptualisation of wave energy converters, physical model testing performed in wave basin laboratories is often applied. In such cases, knowledge about the wave conditions is of great significance. For validation of the wave condition in such tests, different methods for estimation of the directional wave spectra may be applied. However, different assumptions are imposed in the methods and deviations here from provide uncertainties in the results. The following paper quantifies the influence of nonlinear effects on the accuracy of the estimated directional wave spectra. This is done by analysis of idealised, synthetically generated waves based on second order wave theory and secondly with simplified amplitude dispersion included. The present analyses show that the uncertainties of the directional wave spectra are proportional to the level of nonlinearity present in the wave field.

KEY WORDS: Directional wave spectrum; wave analysis; nonlinear waves; MLM; PTPD; second order wave theory; multidirectional waves.

## INTRODUCTION

To meet the increasing demand for renewable energy, the wave energy sector has been in a continuous development the past years. In the development of wave energy converters, it is crucial to know the conditions of the waves to assess the possible power take-off and determine the loads on the structures. Physical model testing is a commonly applied design and validation tool for offshore structures in general. In such tests, the structure is exposed to various short-crested sea states and the structural response is measured.

The generation of waves in laboratory tests can be performed from either Fast Fourier Transform-based approaches like the Random Phase Method or the Random Complex Spectrum, where the energy of the wave spectrum is introduced at discrete frequencies. Alternative, methods based on digital filters may be applied such as the White Noise Filtering Method which may produce continues spectra. To verify if the generated sea state matches the site-specific conditions, analyses of the wave field is required. A variety of methods have been proposed for the analysis of directional wave spectra, among which most aims to determine the Directional Spreading Function (DSF). This type of method includes for instance the Bayesian Directional Method (BDM) (Hashimoto and Kobune, 1988), the Maximum Likelihood Method (MLM) (Capon et al. (1976); Isobe et al. (1984); Krogstad (1988)) and the Extended Maximum Entropy Principal (EMEP) (Hashimoto et al., 1994). Such methods assume a double summation sea state, meaning that each frequency of the irregular wave field has several different directions. Miles and Funke (1989) however found that the double summation model is related with problems regarding phase-locking. The phase-locking causes spatial differences in the energy across the tank, thus a non-ergodic wave field, wherefore it is often preferred to use the single summation model for wave generation in laboratory tests.

The use of FFT-based generation of waves for laboratory tests using the single summation model enables the use of another type of analysis method, where the directional spectrum is estimated based on the direction of each of the generated individual wave components. The Phase-Time-Path-Difference (PTPD) method was given by Esteva (1976) for determination of the direction of propagation for the individual wave components from surface elevation measurements in three non-collinear positions. The directional wave spectrum can then be computed as done by Draycott et al. (2015), which has also been extended to allow for separation in incident and reflected directional wave spectra by Draycott et al. (2016). However, this is under the assumption that the reflections travel in the opposite directions of the incident wave components, which is not valid in presence of structures in short-crested sea states, as at least some of the components will approach the structure from oblique directions.

Common for all of the mentioned approaches is that they are based on linear wave theory, wherefore the surface elevation in position $\vec{x} = [x,y]$ at time $t$ is described by:

$$\eta(\vec{x},t) = \sum_{i=1}^{N} a_i \cos(\omega_i t - k_i[x\cos\theta_i + y\sin\theta_i] + \phi_i) \qquad (1)$$

where:

| | |
|---|---|
| $\eta$ | Surface elevation |
| $a_i$ | Amplitude of the $i^{\text{th}}$ wave component |
| $\omega_i$ | Cyclic frequency of the $i^{\text{th}}$ wave component |
| $k_i$ | Wave number of the $i^{\text{th}}$ wave component by linear wave theory, $\omega_i^2 = gk_i \tanh(k_i h)$ |
| $\theta_i$ | Direction of propagation of the $i^{\text{th}}$ wave component |
| $\phi_i$ | Phase at time $t = 0$ and position $\vec{x} = [0,0]$ of the $i^{\text{th}}$ wave component |
| $g$ | Gravity acceleration |
| $h$ | Water depth |

For the first order theory to be valid, the wave height must be small compared to the water depth and the wavelength, $H/h << 1$ and $H/L << 1$. The validity of wave theories is typically given by the diagram of Le Méhauté (1976). For sea states outside of the linear wave regime, the waves will be nonlinear, and more complicated wave theories will be necessary to accurately describe the waves. The present paper therefore aims to determine the accuracy of the directional spectra estimation when the wave field consists of nonlinear waves, where the description of the waves do not match the mathematical model upon which the analyses are based (Eq. 1).

## Second Order Wave Theory

In the present paper, multidirectional waves of second order wave theory generated based on the procedure given by Schäffer and Stenberg (2003) will be considered. The second order wave theory includes the interaction between pairs of wave components, $\eta_n$ and $\eta_m$, which yields sub- and superharmonic components at the difference and sum frequencies. For interactions between wave components of different direction, the direction of the interactions will also be different, which is illustrated in Fig. 1. This figure illustrates the second order components from a bichromatic wave field consisting of two first order wave components with different directions, $\theta_m^{(1)}$ and $\theta_n^{(1)}$.

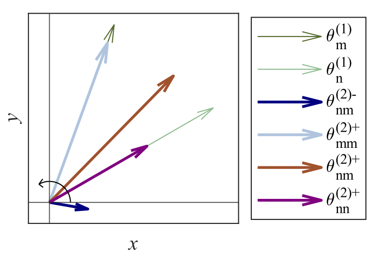


Fig. 1. Vectors indicating the direction and amplitude of wave components of a bichromatic wave field and the corresponding second order components.

As seen in Fig. 1, the superharmonic components due to the interaction between a first order wave component and itself will have similar directions, $\theta_{mm}^{(2)+}$ and $\theta_{nn}^{(2)+}$. For the superharmonic component due to the interaction of two different first order components, the direction hereof will be between the two components, $\theta_{nm}^{(2)+}$, whereas the direction of the subharmonic component will be outside the range of the two original components, $\theta_{nm}^{(2)-}$. This causes, as also found by Sand (1982), an increase in the spreading of the subharmonic components compared to the first order components, when a short-crested, irregular wave field is considered. This is illustrated in Fig. 2, where the mean direction and spreading of two similar wave fields are illustrated, the difference between them being whether the second order contribution is included or not. The directional parameters of a desired sea state in laboratory tests must therefore also reflect the nonlinear behaviour of the wave components to accurately replicate the open sea waves. The level of nonlinearity will in the present analyses be quantified as the amount of second order energy relative to the total amount of energy in the wave field, which will be given as the factor, $\beta$. The amount of second order energy is calculated as the total amount of energy in the second order wave field minus the energy of a similar first order spectrum.

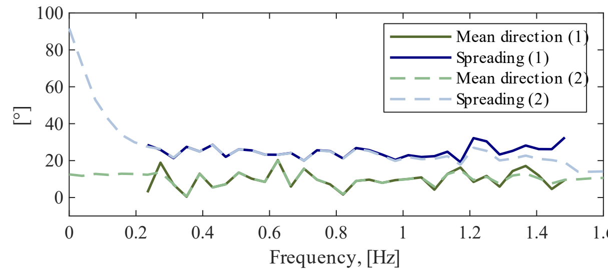


Fig. 2. Directional parameters of wave field based on first order (1) and second order (2) generation.

## Amplitude Dispersion

Waves of second order will have no difference in wave celerity of the primary components compared to the linear dispersion relation and thus only the bound sub and super harmonics travel with a celerity different from the linear dispersion relation. For waves of third order and higher order, amplitude dispersion will however be present and thus the primary components have an increase in celerity. In the present analyses, a simplified amplitude dispersion will be considered, where the relationship between the wavelength of a regular wave, $L_{\text{lin}}$, determined from linear dispersion and the wavelength, $L_{\text{SFWT}}$, determined according to stream function theory is given by the factor, $\alpha$, which is calculated from Eq. 2.

$$\alpha = \frac{L_{\text{SFWT}}}{L_{\text{lin}}} \qquad (2)$$

The factor on the wavelength, $\alpha$, by which the linear wave theory miscalculates the wavelength compared to stream function theory is illustrated in Fig. 3 for regular waves of different steepness and as function of the wave height relative to the water depth. As seen from the figure, the factor on the wavelength increases with increasing steepness and increasing relative wave height.

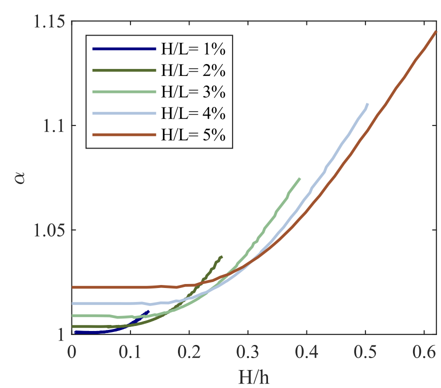


Fig. 3. Estimated error on wavelength based on linear wave theory compared to stream function theory as function of relative wave height for waves of different steepness.

In the present paper, a simplified amplitude dispersion will be added as the factor, $\alpha$, on the wavelengths of all primary components of the considered wave fields. The same factor will be used for the entire spectrum, and the factor will be determined based on the spectral significant wave height, $H_{m0}$, water depth, $h$, and peak period, $T_p$, of the given wave field. This is in agreement with the assumption of Eldrup and Lykke Andersen (2019) for nonlinear long-crested irregular waves.

## METHODOLOGY

### Test Cases

For examination of the performance of the different methods in nonlinear wave fields, a range of test cases have been generated synthetically by single summation. Thus the only deviations from the single summation sea state model is the nonlinearity of the waves. Typical other deviations from the model cover reflections, cross-modes, diffraction and refraction effects, calibration errors on wave gauges etc. The influence of such deviations should similarly be studied separately.

The investigated test cases represent different levels of second order energy in the wave field as well as different levels of simplified amplitude dispersion. Each test case is generated as an irregular wave field with a first order spectrum given as a JONSWAP spectrum with peak enhancement factor, $\gamma = 3.3$. The directional spreading of the wave field is described by a Mitsuyasu-type directional spreading function, $D(\omega,\theta)$, as stated in Eq. (3) with mean direction, $\theta_0 = 10°$, and a spreading parameter, $s = 10$. Time series of surface elevations are generated synthetically for all test cases from an Inverse Fast Fourier Transformation with $N = 4096$ components and a sample frequency of 5 Hz corresponding to a duration of 819.2s.

$$D(\omega,\theta) = \frac{2^{2s-1}\Gamma^2(s+1)}{\pi\,\Gamma(2s+1)}\cos^{2s}\left(\frac{\theta-\theta_0}{2}\right) \tag{3}$$

The individual wave parameters for the test cases are given in Table 1, which furthermore states the amount of second order energy in the wave field, $\beta$. Additionally, the table contains the factor indicating the simplified amplitude dispersion factor, $\alpha$. Note that the cases are reproduced both with and without the simplified amplitude dispersion factor.

Table 1. Sea state parameters of test cases.

| Test Case | $H_{m0}$ [m] | $T_p$ [s] | $h$ [m] | $L_p$ [m] | $\beta$ [-] | $\alpha$ [-] |
|---|---|---|---|---|---|---|
| A | 0.1 | 2 | 2 | 6.06 | 0.001 | 1.003 |
| B | 0.4 | 2 | 2 | 6.06 | 0.007 | 1.039 |
| C | 0.55 | 2.5 | 1.3 | 7.69 | 0.015 | 1.067 |
| D | 0.4 | 2.5 | 0.8 | 6.40 | 0.032 | 1.089 |
| E | 0.45 | 2.8 | 0.8 | 7.31 | 0.051 | 1.112 |
| F | 0.4 | 3 | 0.7 | 7.45 | 0.063 | 1.122 |

The different test cases will be analysed using two of the previously mentioned methods for estimation of the directional wave spectrum. The first being a Maximum Likelihood Estimation of the directional spectrum in standard form, which is among the DSF-reconstruction methods. The other is the Phase-Time-Path-Difference approach, which utilises the knowledge about the generated frequencies in a single summation sea state. The two methods are chosen for the present analysis, as they represent two different types of directional spectrum estimation; a DSF-based approach that fits to the data in a statistical sense based on an assumed shape of the DSF, and the PTPD approach that does not assume any prior knowledge of the shape of the DSF. Furthermore, the two methods differ in the applicability, as the PTPD is only applicable for wave tank tests with single-summation generation applied, whereas the MLM can be applied for open sea measurements. The application of the MLM method to single summation sea states is not in agreement with the assumed DSF unless much more frequencies are included in the generation than in the analysis.

### Maximum Likelihood Estimation of Directional Spectrum Expressed in Standard Form

The Maximum Likelihood Estimation of the Directional Spectrum in Standard Form (MLM) was introduced by Isobe (1990). The method fits to the data in a statistical sense by describing the frequency-dependent Directional Spreading Function (DSF) by a mean direction, $\theta_0$, and a spreading parameter, $s$. The two unknown parameters are fitted to wave data measurements from several gauge positions using the known relationship between the DSF, $D(\omega,\theta)$, and the measured cross-spectra of the wave fields in two positions $\overrightarrow{\boldsymbol{x}_m}$ and $\overrightarrow{\boldsymbol{x}_n}$ as stated in Eq. (4). All possible gauge pairs are then used for the fitting of the parameters, $s$ and $\theta_0$.

$$\frac{S_{\eta_n\eta_m}(\omega)}{S_{\eta\eta}(\omega)} = \int_{-\pi}^{\pi} D(\omega,\theta)\exp(-\mathrm{i}\vec{\boldsymbol{k}}(\overrightarrow{\boldsymbol{x}_n}-\overrightarrow{\boldsymbol{x}_m}))\,\mathrm{d}\theta \tag{4}$$

where:
$\vec{\boldsymbol{k}}$ Wave number vector, $\vec{\boldsymbol{k}} = k[\cos\theta\,;\sin\theta]$

The DSF, $D(\omega,\theta)$, used in the MLM analyses is similar to the one, upon which the test cases are generated, as stated in Eq. (3).

The MLM therefore assumes a directional distribution of the individual frequency components being analysed. For analysis of wave field generated in laboratory facilities using the single summation model, the analysis therefore requires an increase of the frequency increment in the frequency discretization of the analysed spectrum. To utilize the entire time-series of the data set, the entire time-series is divided into a sufficient amount of subseries, wherefore the frequency increment of the analysis will be of equal number times larger than in the generation, such that $\delta f_{\text{MLM-analysis}} = J \cdot \delta f_{\text{generation}}$. Where $J$ is the number of subseries and by use of the entire time-series therefore also the number of generated directions per analysed frequency.

A likelihood-function is suggested by Isobe (1990), which represents the joint probability of obtaining exactly the estimates obtained from the $J$ time-series in the $M$ gauge positions. The likelihood function is given in Eq. (5).

$$L = \frac{1}{(2\pi\Delta f)^M\sqrt{\det(\boldsymbol{\Omega})}}\exp\left(-\frac{1}{2}\sum_{k=1}^{2M}\sum_{l=1}^{2M}\boldsymbol{\Omega}_{kl}^{-1}\widehat{\boldsymbol{\Omega}}_{lk}\right) \tag{5}$$

where:
$M$ Number of wave gauge positions
$\boldsymbol{\Omega}$ Cross spectral density matrix based on the estimated directional parameters
$\widehat{\boldsymbol{\Omega}}$ Measured cross spectral density matrix as average of the J subseries

The likelihood function is then maximised in order to determine the most optimal choice of directional parameters, $\theta_0$ and $s$, which will maximise the probability of obtaining the measured Fourier coefficients. The optimisation is for the present analyses performed using the 0th order method by Nelder and Mead (1965) as a minimisation of the negative likelihood function due to computational reasons.

## Phase-Time-Path-Difference Approach

As mentioned previously, the Phase-Time-Path-Difference Approach utilises that the wave fields are generated based on the single summation model from a Fast Fourier Transform, wherefore each of the wave components has a single direction, that can be calculated from Eqs. (6) and (7) according to Esteva (1976) for wave signals in three non-colinear positions, $(x_1, y_1)$, $(x_2, y_2)$ and $(x_3, y_3)$. In the PTPD approach, the exact same frequency components as those being generated are therefore analysed.

$$\theta = \tan^{-1}\left(\frac{\left[(x_1 - x_2)\phi_{1,3} - (x_1 - x_3)\phi_{1,2}\right]\frac{1}{sgn(Q)}}{\left[(y_1 - y_3)\phi_{1,2} - (y_1 - y_2)\phi_{1,3}\right]\frac{1}{sgn(Q)}}\right) \quad (6)$$

$$Q = (x_1 - x_2)(y_1 - y_3) - (x_1 - x_3)(y_1 - y_2) \quad (7)$$

where:

$\theta$ Direction of propagation of single long-crested wave component

$\phi_{i,j}$ Phase difference between location $i$ and $j$

To estimate the directional wave spectrum from an array of surface elevation gauges, they will be combined in triads as following the procedure given by Draycott et al. (2015), whereafter an overall estimate is determined from the result given by the different triads using the peak of a circular kernel density estimate hereof. Each frequency component in the spectrum of irregular waves is considered individually. The PTPD approach yields the restriction on the wave gauges, that the distance between the gauges in the triads must not exceed half of the wavelength of the considered wave component. In the further extension to the SPAIR method by Draycott et al. (2016), where the PTPD approach is extended to separate the wave field in the incident wave spectrum and the reflected wave field under the assumption that the reflected components travel in the opposite direction of the incident wave components, the limitation on the wave gauge distances is further limited to be $\Delta x > 0.05L$ and $\Delta x < 0.45L$. These criteria will be implemented in the present analyses even though reflections are not present.

The directional wave spectrum is then at last reproduced from the estimated spectral density and direction of propagation of the individual wave components from the measurements. The individual components are added to a corresponding frequency bin with a larger frequency increment, wherefore several frequency components contribute to the same frequency bin, which yields the directional spreading within each frequency bin. The number of components in each frequency bin is chosen as the same number of subseries, $J$, for the MLM analyses, which therefore yields the same target directional wave spectra for each of the methods.

## Gauge Array Design

Common for the methods used in the present paper is that the directional wave spectrum is estimated from wave signals in at least three non-colinear positions using either the cross spectra or phase differences in the different positions. From linear waves measured in two different positions, the direction of propagation of a regular, long-crested wave can be determined within a span of 0º-180º. Measurements from a third non-colinear position is required in order to determine whether the wave travels in one or another direction as illustrated in Fig. 4.

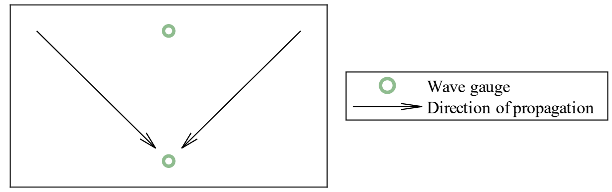


Fig. 4. Possible directions determined from surface elevation measurements in two positions.

When deviations such as second order contributions and simplified amplitude dispersion is included in the wave field, it is expected that the estimated direction will be most accurate for a gauge pair that is placed perpendicular to the direction of propagation of the wave, as the surface elevation signal in that case will be similar in both positions, and the direction can be determined independently of wave celerity or wavelength. For waves from other directions, a celerity difference will lead to a wrong direction being calculated. The orientation of the different gauge pairs in the wave gauge array is therefore expected to be of significant influence for the effect of nonlinearities. The CERC5 gauge array developed by Borgman and Panicker (1970) is used for the present analyses and is illustrated in Fig. 5.

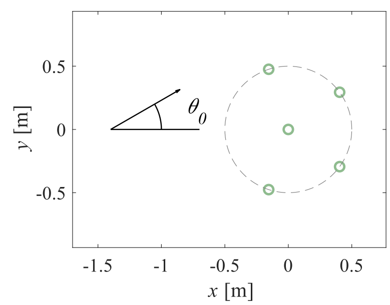


Fig. 5. CERC5 gauge array with diameter 1m.

The CERC5 gauge array is commonly used in for instance the wave basin at Aalborg University, where the wave makers are placed in one side of the basin, being the left-hand side in Fig. 5. Due to the composition of the CERC5 array, the direction of possible gauge pairs is almost evenly distributed from 0º to 180º except two pairs positioned in 90º as illustrated in Fig. 6 As seen from Fig. 5 the two pairs with the same orientation though have different distances. And a similar distribution appears for 180º to 360º when pairing the gauges oppositely.

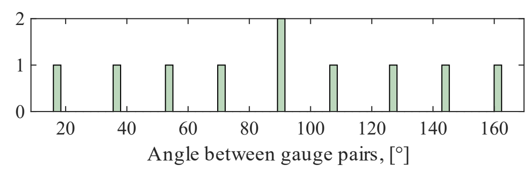


Fig. 6. Directions between possible gauge pairs in CERC5 array.

The distances between the gauge pairs in the CERC5 gauge array design will be either 0.5m, 0.59m or 0.95m due to the symmetry of the array. To evaluate on the gauge array design relative to test cases, the frequencies yielding the limit values of the wavelength for which all gauge distances of the different combinations of triads are valid based on the criteria stated for the PTPD approach are determined. This is similarly the frequencies with the highest reliability of the estimated directional parameters from applying MLM. The ranges are illustrated by the coloured regions in Fig. 7. The solid part of the coloured ranges indicates the frequencies where all gauge distances fulfil $\Delta x > 0.05L$ and $\Delta x < 0.45L$. The dashed coloured range then indicates the range where at least one of the wave gauge pairs fulfil be $\Delta x > 0.05L$ and $\Delta x < 0.45L$. Furthermore, the figure illustrates the truncation of the spectrum with dotted black lines. The spectrum is truncated at 0.5 and 3 times the peak frequency, which is similar to the truncation of the linear spectrum that is used in the generation of the waves.

As seen in Fig. 7, the choice of wave gauge array design corresponds rather well with all the test cases being analysed in the present paper, as the range covering most of the generated spectrum is where all gauge distances are within the desired value relative to the wavelength. However, sub and superharmonics add lower and higher frequencies that may be outside of the separation range. The methods used in the present paper fit to the measured data in a statistical sense. If not all the gauge distances are useful (in the dashed coloured region of Fig. 7), the estimates will be associated with lower statistical accuracy compared to the components inside the range of the solid line. As the present paper considers wave spectra of the JONSWAP type with peak enhancement factor $\gamma = 3.3$, it is assumed that the gauge array design is appropriately scaled for all test cases, as the main part of the energy can be analysed with highest possible statistical accuracy with use of five wave gauges.

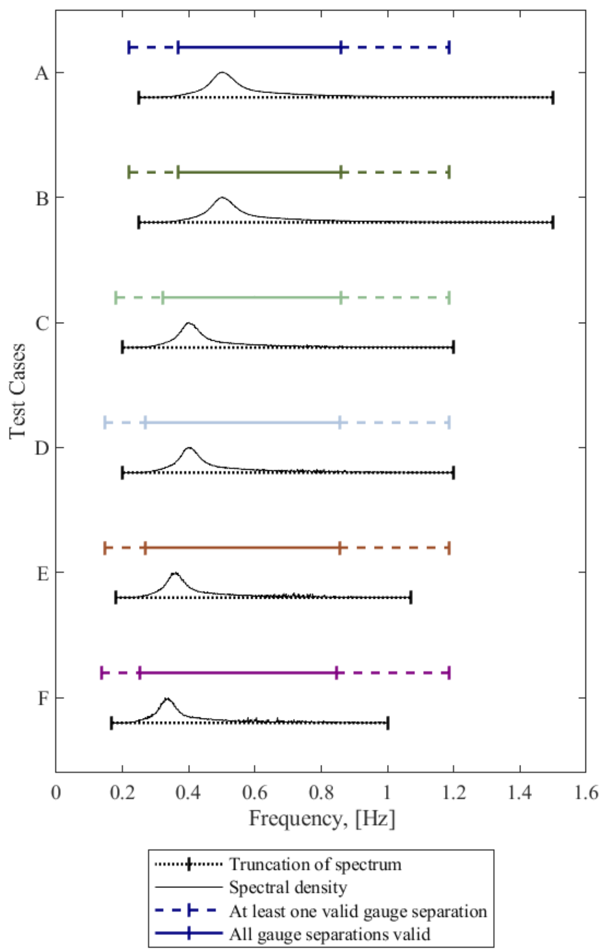


Fig. 7. Validity of wave gauge array according to desired wave gauge distances between $0.05L$ and $0.45L$ for all test cases.

DISCUSSIONS

As the aim of the present analyses is to study the nonlinear effects separately, a target directional spectrum is determined for each of the test cases to be used as the frame of reference. First, the performance of the considered methods is determined based on analyses of the first order components of the wave fields, which is possible due to the use of synthetic data. Next, the wave fields containing the second order contribution as well is analysed. Last, analyses are performed of the wave fields containing the second order contribution as well as the correction of the wavelength of the first order components corresponding to a simplified inclusion of amplitude dispersion. In this manner, the nonlinear effects are studied separately.

For quantification of the performance of the different methods, the Normalised Total Difference (NTD) between the predicted, $S(f,\theta)_{m,pq}$, and target, $S(f,\theta)_{t,pq}$, directional spectra is determined:

$$\mathrm{NTD} = \frac{\sum_{p=1}^{N_f} \sum_{q=1}^{N_\theta} \left| S(f,\theta)_{t,pq} - S(f,\theta)_{m,pq} \right|}{\sum_{p=1}^{N_f} \sum_{q=1}^{N_\theta} S(f,\theta)_{t,pq}} \tag{8}$$

## Method Performance

The method performance is initially evaluated from wave field generated based on first order theory. The estimated directional spectra based on the different methods appear in Fig. 14 in the Appendix along with the target directional spectra. The estimated directional spectra have average deviations of 0.0% for the PTPD approach and 38.7% for the MLM. The deviations for the MLM estimates results in a larger estimated directional spreading compared to the target spectra, cf. Fig. 14. As the MLM assumes a wave field generated from the double summation model, and the analysed wave fields are generated from the single summation model, larger deviations are per default expected. The MLM can though be used for open sea measurements as well, whereas the PTPD approach is only applicable for laboratory tests where the specific generation model is used. Thus, the method performances in the nonlinear wave fields will be considered relative to the performance in the first order wave fields.

## 2nd Order Waves

The nonlinear wave field of the investigated test cases consist of a similar wave field in relation to the random phases applied to each wave component as previously mentioned. In the present analyses, the second order contributions are included. The target spectrum for the second order wave fields therefore also takes the directions of the second order components into account. The difference in NTD between the analysis of the similar first order wave field and the wave field generated based on second order wave theory, $\Delta\mathrm{NTD} = \left|\mathrm{NTD}^{(2)} - \mathrm{NTD}^{(1)}\right|$, will be used to evaluate the method performance by considering the influence of the second order effects only. The relative NTD's for all test cases appear from Fig. 8, where they are illustrated as function of the amount of second order energy in the wave field. $\beta$.

As seen from Fig. 8, the deviation of the directional wave spectra increases with increasing amount of second order energy in the irregular wave field for both methods. For the investigated cases, the deviation increases with up to 5.7 percentage points using the PTPD approach, whereas the deviation increases with up to 9.0 percentage points for MLM for wave fields with approximately 6.5% second order energy. Thus, the accuracy of the estimated directional wave spectra decreases when the nonlinearity of the waves increases.

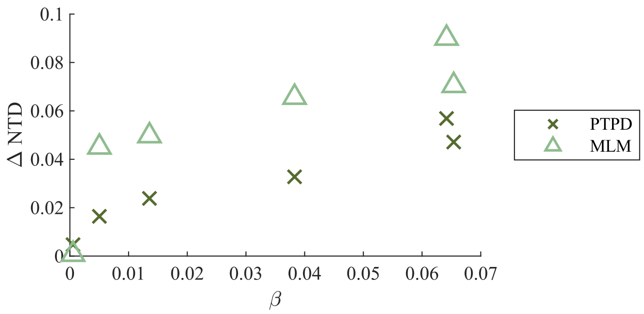


Fig. 8. Relative NTD of directional wave spectra for analysis of second order wave field as function of the amount of second order energy in the wave field, $\beta$.

The distribution of the error of the directional wave spectrum across the different frequencies is illustrated in Fig. 9, which shows the NTD calculated at each frequency for the PTPD analyses of all test cases. From the figure it is clear, that the part of the spectrum with a large amount of first order compared to second order energy is significantly more accurate than the parts of the spectrum dominated by second order energy. This is very clear from the highly nonlinear cases E and F.

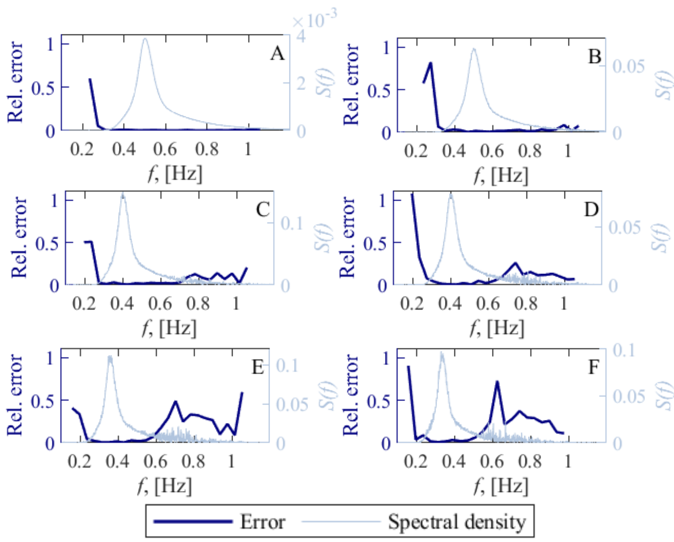


Fig. 9. Error on the estimated directional wave spectrum as distributed over all frequencies for PTPD analysis.

## Simplified Amplitude Dispersion

As mentioned in the description of the wave generation, a simplified amplitude dispersion is included in the wave field by adjustment of the wavelengths of all frequency components by the factor, $\alpha$. The increase in the errors of the estimated directional spectra caused by amplitude dispersion are shown in Fig. 10 for the investigated cases. The baseline for the calculation of ΔNTD is here taken as the tests with 2nd order components included, $\Delta\text{NTD} = \left|\text{NTD}^{(2+\text{amp.disp.})} - \text{NTD}^{(2)}\right|$

The simplified amplitude dispersion does not seem to influence the estimation of the directional spectra gained from the PTPD approach significantly, yielding only an increase in the deviation of 0.3 percentage points for the most nonlinear case. From the results gained from the MLM, the deviation however increases with up to 10.7 percentage points. For the PTPD approach, the inclusion of simplified amplitude dispersion thus seems to have less influence than the inclusion of second order wave components. It seems relevant to consider a more accurate generation of the highly nonlinear waves for further analyses, in which correct amplitude dispersion for irregular waves appears, to clarify if the same behaviour of the methods is experienced as for the simplified amplitude dispersion introduced here.

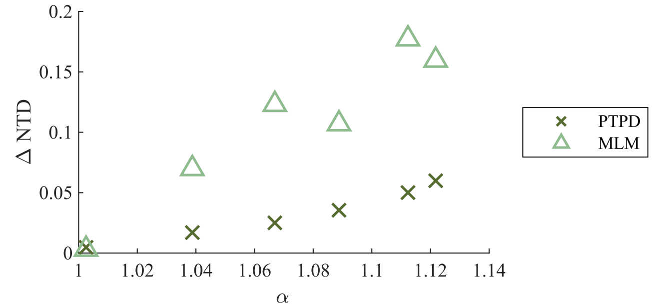


Fig. 10. Relative NTD of directional wave spectra for analysis of wave fields including simplified amplitude dispersion and second order wave components compared to wave fields without simplified amplitude dispersion but with second order wave components as function of the error on the wavelength, $\alpha$.

## Evaluation of Results

Compared to the first order wave fields, the deviations of the directional wave spectra for the investigated test cases are illustrated in Fig. 11 as a function of the error on the wavelength, $\alpha$, for inclusion the combined effects from second order energy and simplified amplitude dispersion.

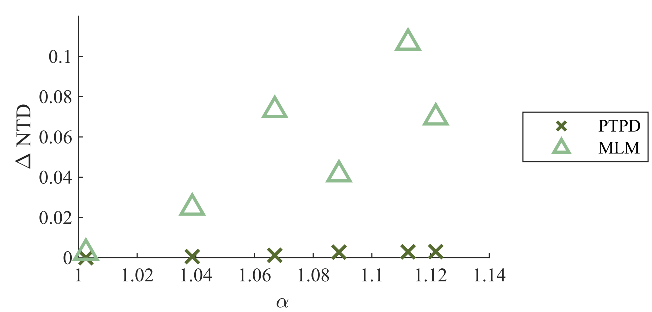


Fig. 11. Relative NTD of directional wave spectra for analysis of second order wave fields including simplified amplitude dispersion as function of the error on the wavelength due to amplitude dispersion, $\alpha$. Here compared to analysis of wave field based on first order wave theory.

A general tendency for both methods similarly shows, that the deviation increases with increasing wave nonlinearity, yielding increases in the deviation with up to 17.2 percentage points for MLM and 6.0 percentage points for the PTPD approach, wherefore improvements of the methods could be considered for future work depending on the desired reliability of the directional spectrum. As the present analyses are performed based on idealised, synthetic data, it should also be expected that the performance decreases further when analysing actual measured data from laboratory or open sea test including further deviations from the mathematical model being for example reflections, cross-modes, diffraction effects, calibration errors on wave gauges etc. The influence on the directional wave spectra is naturally most dominant for the test cases with highest $\beta$ and $\alpha$, wherefore the directional spectra for test case F are illustrated in Fig. 12 and 13. As seen from the figures, and also reflected in the NTD, the influence on the directional spectra estimated from the PTPD approach is less relevant, whereas the directional spectra estimated by MLM show a large increase in the estimated spreading of the waves compared to the target spectrum especially in the superharmonic region.

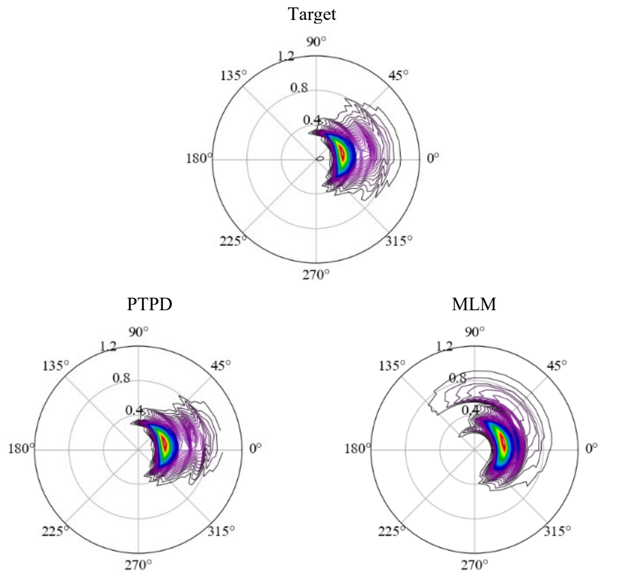


Fig. 12. Target and estimated directional spectra of second order wave fields.

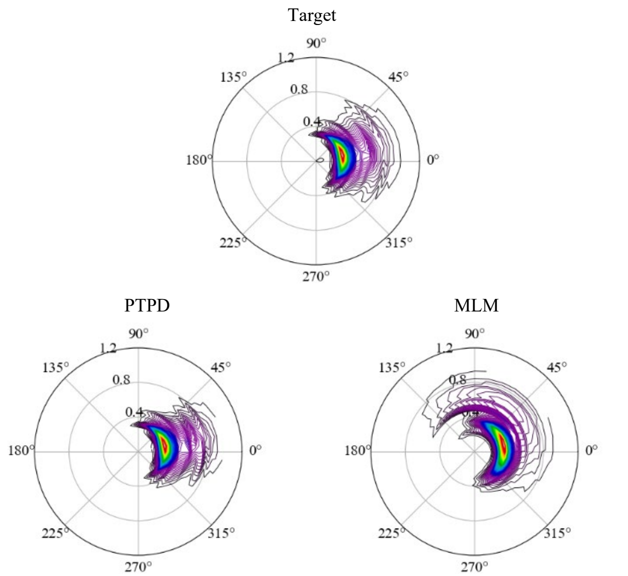


Fig. 13. Target and estimated directional spectra of wave fields with inclusion of simplified amplitude dispersion.

## CONCLUSION

The present paper evaluates the accuracy of estimated directional wave spectra when applying analysis methods based on first order wave theory. The wave fields used in the analysis were generated based on second order wave theory. The analyses were performed on idealised, synthetically generated wave fields with varying amount of second order energy and afterwards with inclusion of simplified amplitude dispersion as well, which made it possible to determine the separate effect of the nonlinear contributions.

The paper demonstrates that for highly nonlinear waves the error of the estimated directional spectra can be significant. The lack of accuracy on the estimated directional wave spectra depends on the level of nonlinearity in the wave field. For waves of second order theory with approximately 6.5% second order energy, the increase in the deviation was up to 5.7 percentage points for PTPD and 9.0 for MLM. For the combined effects investigated for the 6.5% second order energy and simplified amplitude dispersion, the increase in deviation was 6.0 percentage points for PTPD and 17.2 for MLM. Thus, depending on the desired accuracy of the directional wave spectrum, improvement of the methods should be considered.

## ACKNOWLEDGEMENTS

This work was funded by the Danish Energy Agency under The Energy Technology Development and Demonstration Program (EUDP).

## REFERENCES

Borgman, L. E., Panicker, N. N. (1970). “Design Study for a Suggested Wave gage array off Point Mugu, California” Hycraulic Engineering Laboratory, University of California at Berkeley, California. Technical Report 1-14, 117-136.

Capon, J., Greenfield, R. J., Kolker, R. J. (1976). “Multidimensional maximum-likelihood processing of a large aperture seismic array”, *Proc. IEEE,* 55, 192-211.

Draycott, S., Davey, T., Ingram, D. M., Lawrence, J., Johanning, L. (2015). “Using a Phase-Time-Path-Difference Approach to Measure Directional Wave Spectra in FloWave”, *EWTEC Conference Proceedings.*

Draycott, S., Davey, T., Ingram, D. M., Day, A., Johanning, L. (2016). “The SPAIR method: Isolating incident and reflected directional wave spectra in multidirectional wave basins”, *Coastal Engineering*, 114, 265-283.

Eldrup, M. R., Lykke Andersen, T. (2019). Estimation of Incident and Reflected Wave Trains in Highly Nonlinear Two-Dimensional Irregular Waves. Journal of Waterway, Port, Coastal, and Ocean Engineering, Vol. 145, Issue 1 (January 2019).

Esteva, D. (1976). “Wave direction computations with three gage arrays”, *Coastal Engineering Proceedings*, 349-367.

Hashimoto, N., Kobune, K. (1988). “Directional spectrum estimation from Bayesian approach”, *Coastal Engineering Proceedings*, 62-76.

Hashimoto, N., Nagai, T., Asai, T. (1994). “Extension of the maximum entropy principle method for directional wave spectrum estimation”, *Coastal Engineering Proceedings*, 232-246.

Isobe, M., Kondo, K., Horikawa, K. (1984). “Extension of mlm for estimating directional wave spectrum”, *Proc. Sympo. On Description and Modelling of Directional Seas,* A-6.

Isobe, M. (1990). ”Estimation of Directional Spectrum Expressed in Standard Form”, *Coastal Engineering Proceedings,* 1, 467-483.

Krogstad, H. E. (1988). ”Maximum likelihood estimation of ocean wave spectra from general arrays of wave gauges”, *Modelling, Identification and Control*, 9, 373-381.

Le MéHauté, B. (1976). “An Introduction to Hydrodynamics and Water Waves”, Springer.

Miles, M. D., Funke, E. R. (1989). “A Comparison of Methods for Synthesis of Directional Seas”, *J. Offshore Mech. Arct. Eng,* 111(1), 43-48.

Nelder, J. A., Mead., R. (1965). ”A simplex method for function minimization”, *Computer Journal,* 7, 308-313.

Sand, S. (1982). “Long Waves in Directional Seas”, *Coastal Engineering,* 6, 195-208.

Schäffer, H. A., Steenberg, C. M. (2003). “Second-order wavemaker theory for multidirectional waves”, *Ocean Engineering,* 30, 1203-1231.

APPENDIX

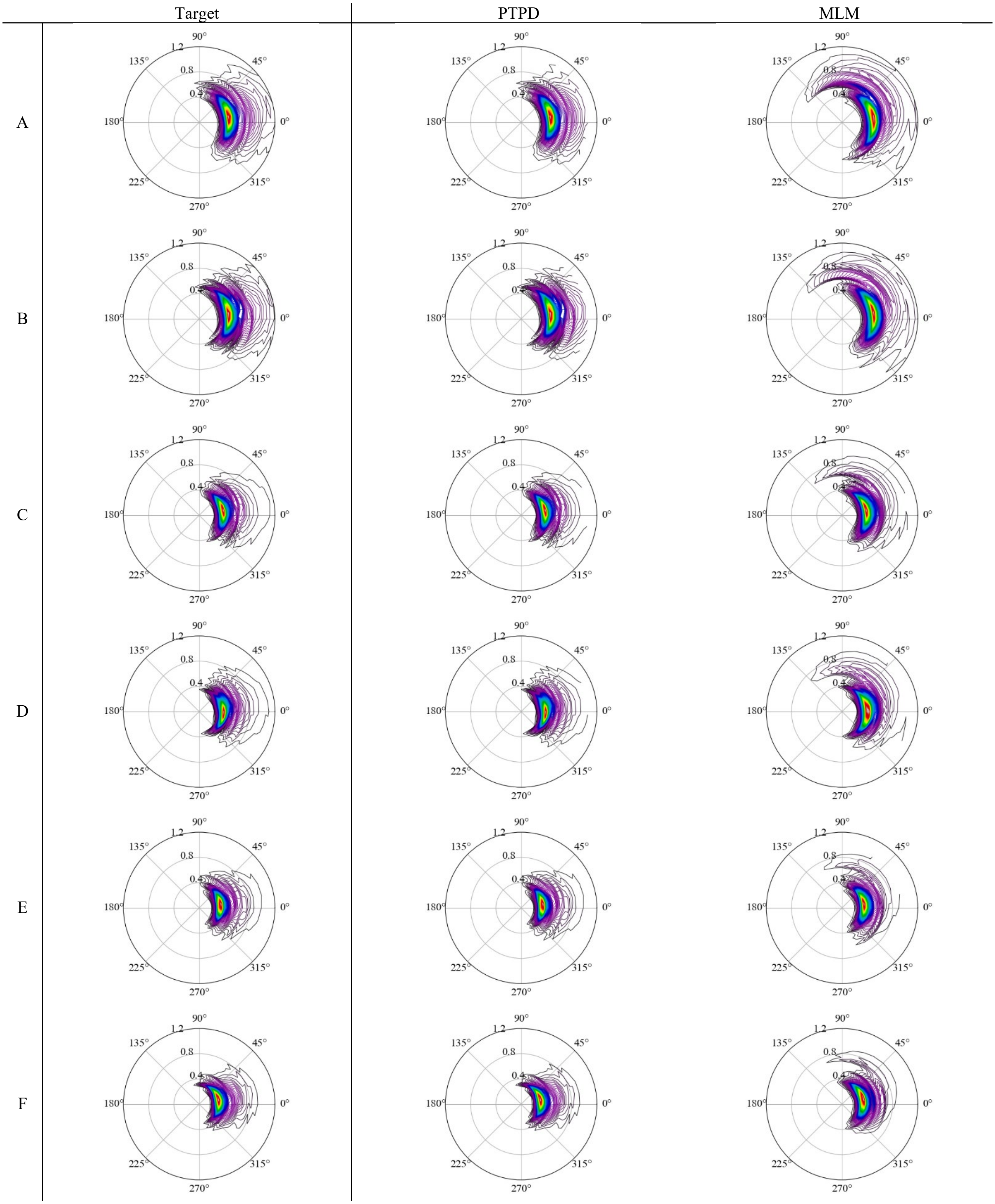

Fig. 14. Target and estimated directional spectra of first order wave fields.